Development of Phase-Separating Microfiber Network Hydrogels to Promote In Vitro Vascularization

Akihiro Nishiguchi[1], Erino Araki[1], Debabrata Palai[1], Shima Ito[1,2], and Tetsushi Taguchi[1,2]*

[1]Biomaterials Field, Research Center for Macromolecules and Biomaterials, National Institute for Materials Science, 1-1 Namiki, Tsukuba, Ibaraki 305-0044, Japan

[2]Faculty of Pure and Applied Sciences, University of Tsukuba, 1-1-1 Tennodai, Tsukuba, Ibaraki 305-8577, Japan

*Corresponding author: Akihiro Nishiguchi, E-mail: NISHIGUCHI.Akihiro@nims.go.jp

Keywords: vascularization, injectable gel, liquid–liquid phase separation, supramolecular chemistry, regenerative medicine

Abstract

Engineered vascularized tissues in vitro exhibit potential for transplantation therapy and disease modeling. Despite efforts to design hydrogels as cell culture platforms for in vitro vascularization, development of vascularized tissues recapitulating the natural structures and functions remains difficult due to poor understanding of the relationship between cellular microenvironments and functions. Herein, we developed microfiber network hydrogels with microporous structures by controlling the liquid–liquid phase separation (LLPS) of proteins and matrix structures in hydrogels. Extracellular matrix protein gelatin was modified with hydrogen-bonding moieties and mixed with hyaluronic acid to form microfiber network structures. Gelatin gelation and hyaluronic acid dissolution led to microporous microfiber network hydrogel formation. Matrix structures of hydrogels were modified by controlling LLPS that affects endothelial cell tube formation. Vascularization was improved using laminin peptides and co-culturing with mesenchymal stem cells. Overall, our approach exhibits potential to induce in vitro vascularization for regenerative medicine and disease modeling applications.

Introduction

In vitro vascularization is a major challenge in tissue engineering.[1] Blood capillary networks of 150–200 μm exist in cells, except in some tissues such as the cartilage, to continuously supply blood containing oxygen and nutrients necessary for human survival.[2] On exceeding the diffusion limit (> 200 μm), cell aggregates cultured in vitro cause hypoxia and necrosis in tissues.[3] Approaches for in vitro vascularization facilitating the transport of substances can aid in the survival of cells in in vitro cultures. Moreover, vascularized tissues exhibit rapid integration into host tissues by connecting with host vasculatures to improve the graft survival.[4] In cell transplantation therapy, slow revascularization of islets post-transplantation (days to weeks) reduces the cell engraftment efficiency.[5,6] To improve the engraftment efficiency, transplantation of vascularized tissues[7] and cells with vascular beds[8] prevents ischemic conditions by ensuring blood supply to transplanted cells and facilitating host integration. Furthermore, vascularized tissues recapitulating the structures and functions of diseased organs and tissues are useful for drug testing and disease modeling. In vitro models with vascular structures are powerful tools to elucidate the pathways associated with vascular disorders and conditions, such as atherosclerosis, stroke, diabetic retinopathy, and cancer.

Hydrogels are key materials for the development of in vitro vascularization technology.[9] Most approaches for the three-dimensional (3D) culture of endothelial cells (ECs) use hydrogel culture platforms, including cell encapsulation,[10] organoid culture,[11,12] micro-molding,[13] 3D-printing,[14] and microfluidic device systems.[15] Hydrogels mediate the physicochemical and biological crosstalk among cells as scaffolds to support EC adhesion, migration, proliferation, and differentiation,[16] leading to enhanced vascularization in vitro.[16] Matrigel is widely used as an angiogenesis-inducing hydrogel. However, as matrigel is obtained from Engelbreth–Holm–Swarm

tumors, it poses the risk of xenogenic and viral contamination. Matrigel contains a mixture of various extracellular matrix (ECM) proteins (14,000 unique peptides and approximately 2,000 unique proteins[17]) and is poorly defined, causing batch-to-batch variability. Furthermore, many uncontrollable parameters, including variable gelation kinetics, degradation profile, and integration with host tissues, limit its clinical use in regenerative medicine.[18] Xenogenic-free cell culture platforms are used as chemically defined synthetic or semi-synthetic hydrogel alternatives. However, these hydrogels often possess densely crosslinked polymer networks with nanoporous structures (e.g., poly(ethylene glycol) hydrogels possess approximately 20 nm pores[19]) that impair cell migration and rapid integration into host tissues.[20] Several approaches using porogens,[21] granular hydrogels,[22] and protein-based hydrogels[23] have been used for cell encapsulation in pore-forming or porous hydrogels. However, these approaches have various limitations, such as the presence of only a few interconnected pores and void spaces for cell migration, tube formation, and cell infiltration in the host. Therefore, hydrogels with structure-controlled matrices are urgently needed for in vitro vascularization.

In this study, we developed cell-encapsulating and microfiber-forming hydrogels for efficient in vitro vascularization (Figure 1). Using a unique system to control the matrix microstructures in hydrogels based on liquid–liquid phase separation (LLPS),[24] microfiber network (μFN) hydrogels were developed. Tendon-derived gelatin (tG) modified with hydrogen-bonded 2-ureido-4[1H]-pyrimidinone (UPy) units (tGUPy) induced LLPS when mixed with hyaluronic acid (HA) to form microfiber structures. tGUPy was further modified with thiol and vinyl sulfone groups (tGUPyTH and tGUPyVS, respectively) to form μFN hydrogels. Various processes (LLPS, tGUPy gelation, and HA dissolution) led to microporous μFN hydrogel formation under cell culture conditions. The matrix microstructures in hydrogels were controlled using LLPS. Furthermore, the

relationships between the matrix microstructures and EC tube formation were investigated. Additionally, whether modifying the hydrogels with laminin-mimetic peptides or co-culturing them with mesenchymal stem cells (MSCs) supports EC tube formation was assessed.

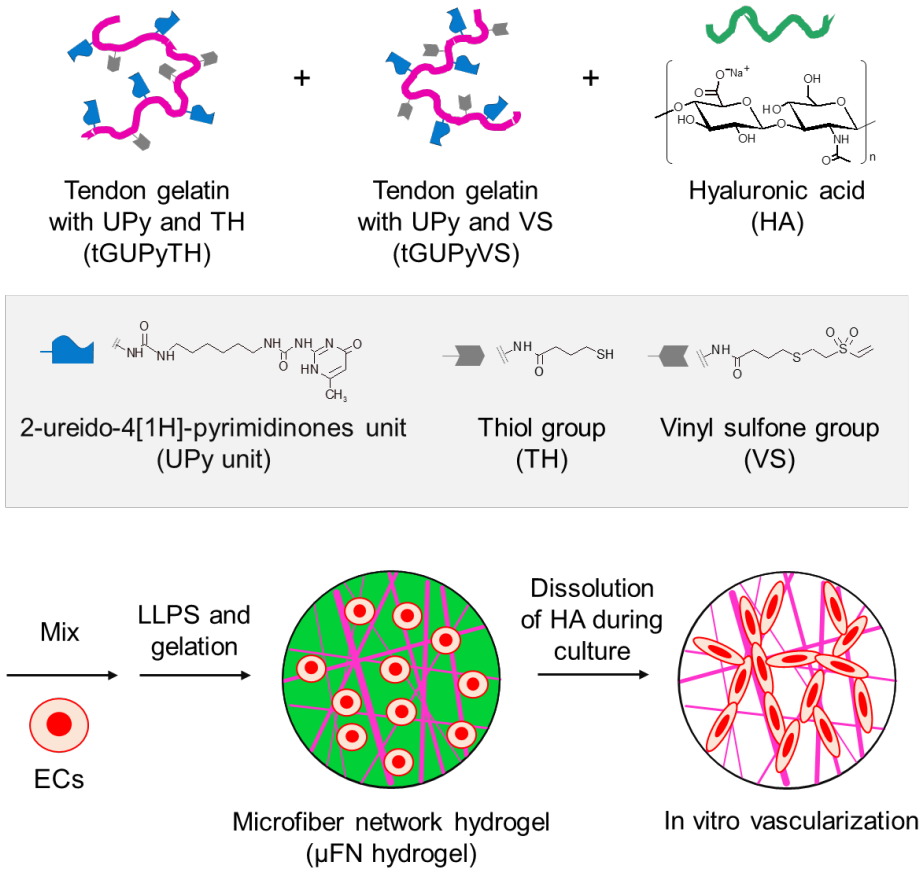

Figure 1. Schematic illustration of the preparation of injectable hydrogels composed of microfiber networks (μFNs) via liquid–liquid phase separation (LLPS). Tendon-derived gelatin (tG) modified with the ureidopyrimidinone (UPy) unit and thiol and vinyl sulfone groups (tGUPyTH and tGUPyVS, respectively) was mixed with hyaluronic acid (HA) to fabricate μFN hydrogels.

Experimental Section

Synthesis of UPy Unit

UPy unit was synthesized as previously described.[25] Briefly, 2-amino-4-hydroxy-6-methylpyrimidine (33.0 mmol, 4.1 g; Sigma-Aldrich, USA) was dispersed in 1,6-diisocyanatohexane (148.6 mmol, 25.0 g; Tokyo Chemical Industry Co., Ltd., Japan). The reaction was performed at 100 ℃ for 16 h under stirring. After cooling to 25 ℃, 10 volumes of hexane were added to precipitate the product. The precipitate was collected via filtration and washed thrice with n-hexane. The product was vacuum dried to obtain UPy units with isocyanate groups.

Synthesis of Gelatin Derivatives

Porcine skin-derived gelatin (sG) and tG (Nitta Gelatin, Inc., Japan) were used to synthesize gelatin derivatives, including sG modified with UPy unit (sGUPy), tGUPy, sG modified with thiol group (sGTH), sG modified with vinyl sulfone group (sGVS), tGUPyTH, and tGUPyVS. sGUPy, tGUPy, sGTH, and sGVS were synthesized as previously described.[26] Additionally, tGUPyTH and tGUPyVS were newly synthesized. To synthesize sGUPy and tGUPy, sG and tG (amino group: 350 μmol/g in sG and 298 μmol/g in tG) were reacted with UPy unit (45% equivalent to the amino groups in sG and tG) in dimethyl sulfoxide (DMSO; 6 wt% for sG and 4 wt% for tG) at 50 ℃ under stirring for 24 h. The products were purified via precipitation with 20 volumes of a cold solvent mixture of ethanol and ethyl acetate (*v*/*v*=1/1) and washed with ethanol. The products were vacuum dried to obtain sGUPy and tGUPy. The number of amino groups was measured using the 2,4,6,-trinitrobenzensulfonic acid assay (Tokyo Chemical Industry Co., Ltd.) to estimate the degree of substitution (DS) of the UPy unit, as previously described.[27]

To synthesize sGTH and tGUPyTH, sG and tGUPy (amino group: 350 μmol/g in sG and 298 μmol/g in tGUPy) were reacted with γ-thiobutyrolactone (200 mol% equivalent to the amino groups in sG or tGUPy; Sigma-Aldrich) in DMSO (6 wt% for sG and 4 wt% for tGUPy) at 50 ℃ under stirring for 24 h. After the addition of tris(2-carboxyethyl)phosphine hydrochloride (TCEP-HCl; 1 mM; Nacalai Tesque, Inc., Japan), the products were purified via precipitation with 20 volumes of a cold solvent mixture of ethanol and ethyl acetate (*v*/*v*=1/1) and washed with ethanol. The products were vacuum dried to obtain sGTH and tGUPyTH. DS of the thiol groups was calculated using Ellman's method.

To synthesize sGVS and tGUPyVS, sGTH (thiol group: 225 μmol/g) and tGUPyTH (thiol group: 60 μmol/g) were dissolved in ultra-pure water (1 wt%) at 50 ℃ under stirring. Divinyl sulfone (200 mol% equivalent to thiol groups in sGTH and tGUPyTH; Tokyo Chemical Industry Co., Ltd.) was added to the solution. The reaction was performed at 50 ℃ for 24 h with stirring. After adding TCEP (1 mM) to the solution, the products were dialyzed in ultrapure water using a dialysis membrane (molecular cutoff: 10 kDa) for three days. After freeze-drying, sGVS and tGUPyVS were obtained.

Synthesis of Fluorescently Labeled Gelatin Derivatives

tG-fluorescein, sGTH-fluorescein, sGUPy-Cy5.5, and tGUPy-Cy5.5 were synthesized as previously described.[24] Briefly, tGUPyTH-Cy5 was synthesized by reacting tGUPy-Cy5.5 with thiobutyrolactone in the same manner as described above. To synthesize HA (Seikagaku Corporation, Japan) modified with fluorescein (HA-fluorescein), HA was dialyzed against 0.1 M HCl overnight, followed by dialysis against distilled water thrice for one day each and freeze-drying to obtain acidic HA. Acidic HA (800 μmol) was dissolved in DMSO (64 mL) overnight,

and 1-ethyl-3-(3-dimethylaminopropyl)carbodiimide (160 μmol; Dojindo, Japan), *N*-hydroxysuccinimide (160 μmol; Fujifilm Wako, Japan), and fluorescein amine (8 μmol) were added to the solution. After stirring overnight at 25 ℃, the products were dialyzed against 0.01 M NaOH thrice for one day each. After dialysis against distilled water twice for two days each, the products were freeze-dried to obtain HA-fluorescein.

Preparation of μFN Hydrogels

tGUPyTH and tGUPyVS were dissolved in phosphate-buffered saline (PBS) at 10 wt% at 50 ℃ under stirring. HA was dissolved in PBS (2 wt%) at 25 ℃ under stirring. The pH was maintained at 7.8, 6.4, and 7.4 using 1 M NaOH, and the solution was kept at 37 ℃ until use. Solutions of tGUPyTH (100 μL), tGUPyVS (100 μL), and HA (200 μL) were vigorously mixed using a pipette. The turbid solution was placed on a substrate and incubated at 37 ℃ for 30 min to obtain μFN hydrogels. To prepare the non-porous hydrogels, a solution of tGUPyTH (100 μL), tGUPyVS (100 μL), and PBS (200 μL) was used. Each fluorescently labeled gelatin derivative was used to visualize the LLPS structure. The samples were observed using CLSM 900 with Airyscan2 (Zeiss, Germany). The fibrous structures of FN hydrogels were observed using a scanning electron microscope (JCM-7000 NeoScope; JEOL, Japan). The samples were sputtered with platinum and observed at an accelerating voltage of 10 kV.

Rheological Measurement

Rheological measurements were performed using a rheometer (MCR301; Anton Paar GmbH, Graz, Austria). Solutions of tGUPyTH (100 μL), tGUPyVS (100 μL), and HA (200 μL) were vigorously mixed using a pipette. The turbid solution was placed on the stage of the rheometer (pre-warmed to 37 ℃) to form μFN hydrogels. A jig with a diameter of 10 mm was placed in a

gap of 1 mm. Time-dependent changes in rheological properties were assessed at 37 ℃ at an angular frequency of 10 rad/s with 1% strain in the oscillatory mode.

Degradation Test

A pre-gel solution (100 μL) of μFN hydrogels was added to a 2-mL tube. After gelation at 37 ℃ for 1 h, PBS (1 mL) with collagenase (1 mg/mL, 120 U/mL) was added and incubated at 37 ℃ for 1, 4, 8, and 24 h. After discarding the supernatant, ultrapure water was added and incubated at 25 ℃ for 1 h for desalination. The resulting gels were freeze-dried and weighed.

Cell Encapsulation in Hydrogels

For sterilization, tGUPyTH, tGUPyVS, and HA were filtered and freeze dried. tGUPyTH and tGUPyVS were dissolved in PBS (10 wt%) at 50 ℃ under stirring. HA was dissolved in PBS (2 wt%) at 25 ℃ under stirring. The solution was maintained at 37 ℃ until further use. Human umbilical vein ECs (HUVECs; Lonza, Switzerland) were cultured in EGM-2 (Lonza, USA). Human bone marrow-derived MSCs (Lonza, Switzerland) were cultured in the Dulbecco's modified Eagle’s medium (Thermo Fisher Scientific, USA) supplemented with 15% fetal bovine serum (Sigma-Aldrich) and 1% penicillin/streptomycin (Thermo Fisher Scientific). HUVECs and MSCs were harvested via trypsin treatment and collected as pellets after centrifugation at 1200 rpm for 5 min. After removing the supernatant, a mixture of tGUPyTH, tGUPyVS, and HA (volume ratio 1:1:2) was added to the cell pellet and mixed using a pipette. After incorporating the YIGSRC peptide (Peptide Institute, Inc., Japan), the stock solution (50 mM, PBS) was added to the cell suspension, and the final concentration was set to 1.25 mM. Then, HUVECs (4×10^5) were encapsulated in 20 μL hydrogels for monoculture, and HUVECs (2×10^5) and MSCs (2×10^5) were encapsulated in 20 μL hydrogels for co-culture. The mixture was placed on a chamber cover

(10 × 10 mm). The chamber was turned over and incubated at 25 ℃ for 30 min for gelation. Then, the medium (400 μL) was added and cultured for 1–2 d at 37 ℃ in a 5% CO_2 incubator.

Fluorescence Staining

Cells were fixed with 4% paraformaldehyde for 30 min. After washing with PBS, the cells were permeabilized with 0.2% Triton-X for 30 min and blocked with 1% bovine serum albumin/PBS for 1 h. For actin staining, cells were stained with rhodamine-labeled phalloidin (1:200; Thermo Fisher Scientific) overnight at 4 ℃. After washing with PBS, the nuclei were stained with 4',6-diamidino-2-phenylindole (Thermo Fisher Scientific) for 1 h. The samples were observed via confocal laser scanning microscopy (CLSM), and the cell area was quantified using the ImageJ software.

Biodegradability Test

All animal experiments were approved by the Animal Care and Use Committee of the National Institute for Materials Science. sGTH, sGVS, and tG or tGUPy were mixed at 1:1:2 volume ratio, placed in a silicone mold of 1 mm thickness, and incubated at 37 °C for 1 h. Seven-week-old female C57BL/6J mice (Jackson Laboratory, USA) were anesthetized via inhalation of 2% isoflurane. Hair was shaved from the backs of the mice, and the shaved areas were disinfected with 70% ethanol. Hydrogels were subcutaneously implanted into the backs of mice. At 1, 2, 3, and 7 d after implantation, the mice were euthanized via blood removal, and their tissues were collected. The samples were fixed with 10% formalin buffer solution for three days and sectioned. After staining with hematoxylin and eosin, the stained section images were scanned using a digital slide scanner (NanoZoomer S210; Hamamatsu Photonics, Hamamatsu, Japan).

Statistical Analyses

Results are expressed as the mean ± standard deviation. One-way analysis of variance followed by Tukey's multiple-comparison *post-hoc* test was used to compare the differences among groups. Experiments were repeated multiple times as independent experiments. Data shown in each figure are complete datasets obtained from independent representative experiments. No sample was excluded from analysis. Statistical significance is indicated by $*P < 0.05$, $**P < 0.01$, $***P < 0.001$, and $****P < 0.0001$. Statistical analyses were conducted using the GraphPad Prism software (version 8.0; GraphPad Software).

Results and Discussion

Formation of Microfiber-Based Hydrogels via LLPS

Gelatin derivatives were synthesized to prepare the LLPS hydrogels (Table 1). UPy units exhibit associative interactions via quadruple hydrogen bonding in UPy dimers.[25,28] Using this self-associating property of UPy units, tGUPy induces LLPS when mixed with other polymers. To confirm LLPS, tGUPyTH and tGUPyVS were dissolved in PBS at 10 wt% and mixed with 2 wt% HA solution to form μFN hydrogels. HA is an ECM-derived glycosaminoglycan with immunomodulatory functions.[29] After LLPS, chemical crosslinking via thiol-ene reaction between tGUPyTH and tGUPyVS produced mechanically stable hydrogels. CLSM revealed that a mixture of tGUPyTH, tGUPyVS, and HA (tGUPyTH + tGUPyVS + HA) formed microfibrous LLPS structures in hydrogels, whereas no LLPS occurred without UPy units (tGTH + tGVS + HA; Figure 2a). The microfiber network structures of tGUPy were three-dimensionally distributed in the hydrogels, and HA was present around the fibers (Figure 2b). Formation of μFN structures in hydrogels was also confirmed by scanning electron microscopy (Figure 2c). Rheological measurements showed that gelation was initiated after mixing the polymers and reached 60 Pa after 30 min (Figure 2d). To evaluate their biodegradability, the hydrogels were treated with collagenase (Figure 2e). μFN hydrogels exhibited a gradual decrease in weight and almost completely degraded after 24 h of incubation. As hydrogels are composed of ECM proteins and gelatin, they are enzymatically degraded by collagenase. Histological observation of μFN hydrogels after subcutaneous implantation in mice revealed that the hydrogels were degraded within seven days (Figure 2f) via cellular infiltration into the microporous structures or enzymatic degradation.

Table 1. Synthesis of gelatin derivatives.

	Amino groups in tG[a]	UPy-NCO	γ-Thiobutyrolactone	Divinyl sulfone	UPy[a]	TH[b]	VS[b]	DS of UPy[b]	DS of TH[b]	DS of VS[b]	Molecular weight	Yield
	(μmol/g)	(eq. to amino groups)	(eq. to amino groups)	(eq. to amino groups)	(μmol/g)	(μmol/g)	(μmol/g)	(%)	(%)	(%)	(kDa)	(%)
tG	263	0	0	0	-	0.2	-	-	0.1	-	275	-
tGUPy	263	45	0	0	97	0.3	-	37	0.1	-	223	88
tGUPyTH	263	45	2	0	97	60	-	37	23	-	220	97
tGUPyVS	263	45	0	2	97	8	52	37	3	20	197	105

[a]Amino groups in as-prepared tendon-derived gelatin (tG) were assessed by determining the residual amino groups using 2,4,6,-trinitrobenzensulfonic acid (TNBS).

[b]Thiol groups in tG and degree of substitution (DS) values of thiol and vinyl sulfone groups were calculated using Ellman's method.

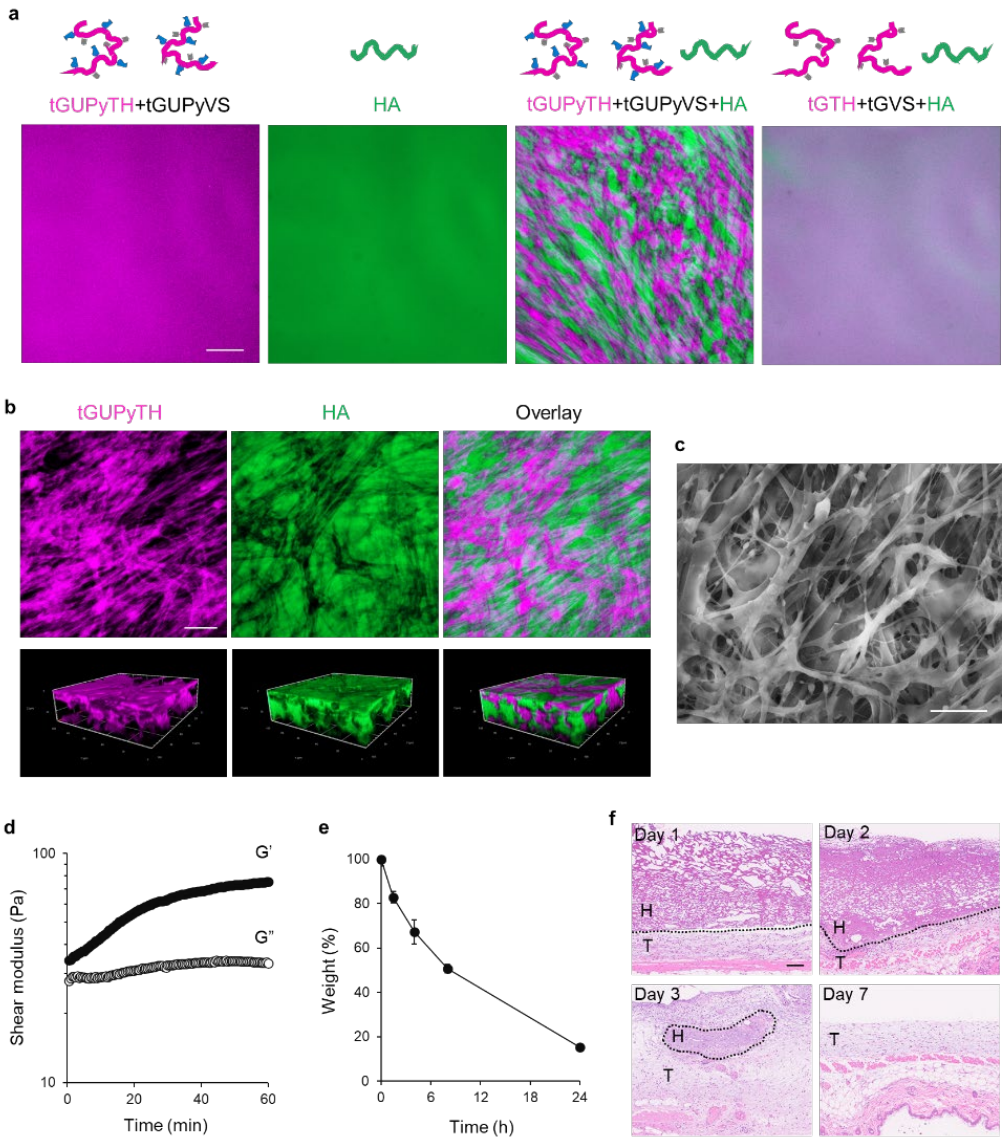

Figure 2. (a) Confocal laser scanning microscopy (CLSM) images of the LLPS structures of tGUPyTH + tGUPyVS, HA, tGUPyTH + tGUPyVS + HA, and tGTH + tGVS + HA. tGUPyTH and tGTH were fluorescently labeled with Cy5.5 (violet), and HA was labeled with fluorescein (green). (b) 3D-reconstructed CLSM images of μFN hydrogels. (c) Scanning electron microscopy (SEM) image of μFN hydrogel. (d) Time-dependent shear modulus change in μFN hydrogels. (e) Degradation test of μFN hydrogels (n = 3). (f) Hematoxylin and eosin (H&E) images of μFN hydrogels on day 1, 2, 3, and 7 after subcutaneous implantation in mice. H and T denote the hydrogel and tissue, respectively. Scale bars represent 50 μm in (a and b), 10 μm in (c), and 100 μm in (f).

Control of LLPS in μFN Hydrogels

Next, we investigated the effect of polymer solution concentration on LLPS in hydrogels. LLPS is of three types: simple coacervation, associative, and segregative LLPS.[30] In tGUPy-HA, segregative LLPS was observed due the strong intermolecular hydrogen bonding between UPy units of tGUPy. LLPS occurs due to intermolecular interactions and is dependent on the polymer concentration and ratio. At the highest concentrations of tGUPy (5 wt%) and HA (1 wt%), μFN structures were formed, with a diameter thinner than that of other LLPS structures (Figure 3a and b). When HA concentration was decreased, fiber diameter increased and the mixture of 2.5 wt% tGUPy and 0.5 wt% HA showed the highest diameter with gyroid-like structures. Below 2.5 wt% tGUPy, LLPS structures consisted of short fibers or droplets. These results are consistent with a previous report that the intensity of intermolecular interactions and viscosity of tGUPy affect the LLPS structures.[24] As the increase in concentration enhances the interaction and viscosity of tGUPy, microfiber structures formed by applying shear stress did not fuse, leading to the maintenance of thin fiber structures. These results suggest that LLPS structures can be controlled by adjusting the polymer concentration and mixture ratio.

To understand the mechanism of LLPS formation, the effects of different types of polysaccharides on LLPS formation were investigated (Figure 2c). Alginate showed a similar morphology to HA, whereas dextran exhibited a thick and droplet-like morphology, partially due to the intensity of the interaction between tGUPy and polysaccharide and viscosity of the polysaccharide solution. Competitive inhibition test using urea revealed that the addition of 1 M urea to μFN hydrogels changed the LLPS structures from fibers to droplets (Figure 2d). When 10 M urea was added, the LLPS structures completely disappeared, and the mixture of tGUPy and HA was miscible.

Therefore, intermolecular hydrogen bonding is the main driving force for LLPS structure formation.

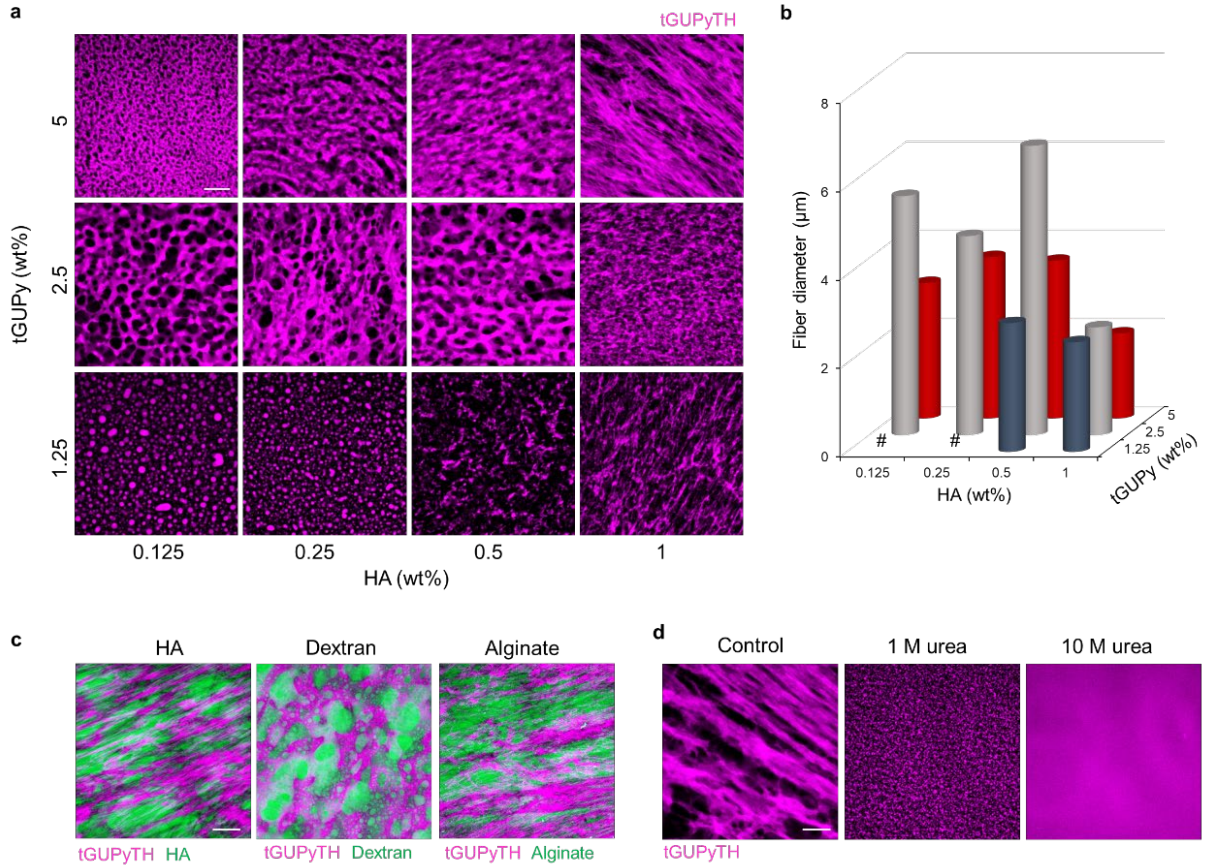

Figure 3. (a) CLSM images of the LLPS structures of hydrogels. The concentrations shown here are the final concentrations of polymers in the hydrogels. tGUPyTH was fluorescently labeled with Cy5.5 (violet). (b) Fiber diameters of the hydrogels. Diameter was measured using CLSM images, and 50 fibers were counted. # indicates no fiber formation, except droplets. (c) Effect of polysaccharide structure on LLPS structure. tGUPyTH-Cy5.5, HA-FITC, Dex-FITC, and Alginate-FITC were used for visualization. (d) Competitive inhibition of μFN hydrogel formation using 1 and 10 M urea. Scale bars represent 50 μm.

Vascularization in LLPS Hydrogels

To clarify the effect of the matrix microstructure on vascularization, various LLPS hydrogels were generated and used for the encapsulation of ECs. Here, five types of hydrogels (non-microporous, μFN, microcapillary network [μCN], gyroid, and droplet) were prepared using different combinations of gelatin derivatives (tGUPy, tGUPyTH, tGUPyVS, sGTH, sGVS, and sGUPy) and HA (Figure 4a). CLSM revealed that μFN hydrogels (tGUPyTH + tGUPyVS + HA) formed fiber network structures after immersion in PBS via dissolution of HA, whereas hydrogels without GUPy exhibited non-porous structures (tGUPyTH + tGUPyVS). To assess the inverse structure of μFN hydrogels, μCN hydrogels were prepared using sGTH + sGVS for crosslinking and GUPy as a porogen. The fiber diameter was tuned by varying the gelatin derivatives (sGUPy or tGUPy), which changed the self-association properties and formed gyroid-like structures. Droplet LLPS hydrogels were prepared by decreasing the tGUPy concentration. The porosity of μFN, μCN, and gyroid hydrogels after immersion in PBS was approximately 50%, which correlated with the volume of GUPy solution (Figure 3c).

Next, ECs were encapsulated in these LLPS hydrogels and their morphologies were observed (Figure 3d). CLSM images revealed that μFN hydrogels possessed the highest area of cellular spreading of ECs compared to the other hydrogels (Figure 3e). In non-microporous hydrogels, ECs did not adhere to the round morphology. Previously, we reported that CN hydrogels facilitate the spread of MSCs.[24] However, in this study, EC spreading and tube formation were limited in μCN hydrogels similar to that observed in gyroid and droplet hydrogels. Localization of ECs on μFN structures was observed via CLSM, and ECs directly adhered to the fiber-like hydrogels and exhibited spreading (Figure 3f). These results suggest that μFN hydrogels promote tube formation

of ECs by improving the mass transport through micropores and providing biomimetic fibrous adhesive scaffolds.

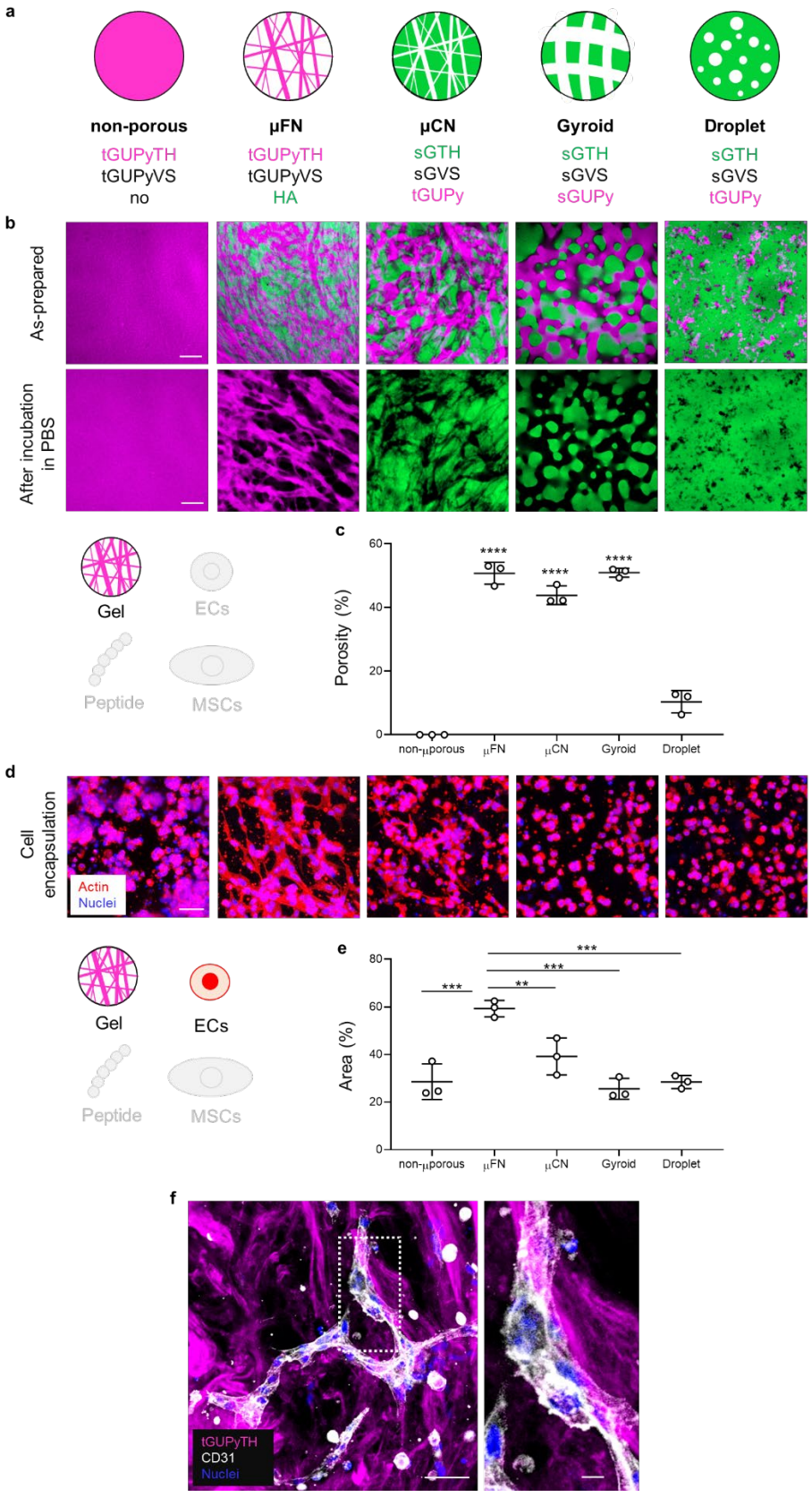
a
non-porous
tGUPyTH
tGUPyVS
no
μFN
tGUPyTH
tGUPyVS
HA
μCN
sGTH
sGVS
tGUPy
Gyroid
sGTH
sGVS
sGUPy
Droplet
sGTH
sGVS
tGUPy
b
As-prepared
After incubation in PBS
Gel
ECs
Peptide
MSCs
c
Porosity (%)
non-μporous
μFN
μCN
Gyroid
Droplet
d
Cell encapsulation
Actin
Nuclei
Gel
ECs
Peptide
MSCs
e
Area (%)
non-μporous
μFN
μCN
Gyroid
Droplet
f
tGUPyTH
CD31
Nuclei

Figure 4. (a) Schematic of LLPS hydrogels: non-microporous, μFN, microcapillary network [μCN], gyroid, and droplet hydrogels. (b) CLSM images of hydrogels formed via no LLPS (non-microporous), associative LLPS (μFN), and segregative LLPS (μCN, gyroid, and droplet). tGUPyTH-Cy5.5, HA-FITC, tG-FITC, sGTH-FITC, sGUPy-Cy5.5, and tGUPy-Cy5.5 were used for visualization. (c) Porosity of LLPS hydrogels (n = 3). ****$P < 0.0001$ compared with non-microporous and droplet hydrogels. (d) CLSM images of endothelial cells (ECs) encapsulated in hydrogels. ECs were encapsulated in hydrogels and cultured for 24 h. Actin and nuclei were stained with phalloidin (red) and 4',6-diamidino-2-phenylindole (DAPI; blue), respectively. (e) Quantification of EC area in hydrogels. (f) Localization of ECs and μFN structures in hydrogels. CD31 and nuclei were stained with the anti-CD31 antibody (white) and DAPI (blue), respectively. Data are represented as the mean ± standard deviation (SD) from a representative experiment (biologically independent samples). *$P < 0.05$ and ***$P < 0.001$ analyzed via one-way analysis of variance (ANOVA) with Tukey's multiple-comparison *post-hoc* test. Scale bars represent 50 μm in (b, d, and f) and 10 μm in (inset of f).

Peptide Functionalization and Co-Culture with MSCs

We further assessed the improvement in vascularization via peptide functionalization of the hydrogels and co-culture with MSCs. YIGSR peptide is a laminin-mimetic peptide that accelerates cellular adhesion.[31] Here, YIGSRC peptides were chemically modified with hydrogels via the reaction between thiol groups in the cysteine residue of peptides and vinyl sulfone groups in sGVS (Figure 5a). CLSM revealed the spread and tubular structures of ECs in the YIGSRC peptide-modified nonporous hydrogels, indicating that the peptides support cellular adhesion and tube formation (Figure 5b). In contrast, cellular spreading improved insignificantly, and the effect of LLPS-induced porous structures was more dominant when ECs were encapsulated in YIGSRC peptide-modified μFN hydrogels (Figure 5c). To support the vascularization of ECs, they were co-cultured with MSCs. MSCs induce angiogenesis by secreting angiogenic factors, such as vascular endothelial growth factors, via the paracrine pathway,[32] thus promoting vascularization (Figure 5d). Co-culture of ECs with MSCs enhanced the tube formation in μFN hydrogels compared to that in non-microporous hydrogels (Figure 5e and f). However, tube formation was not substantially enhanced with peptide modification alone, indicating that the matrix microstructure in hydrogels enhances vascularization.

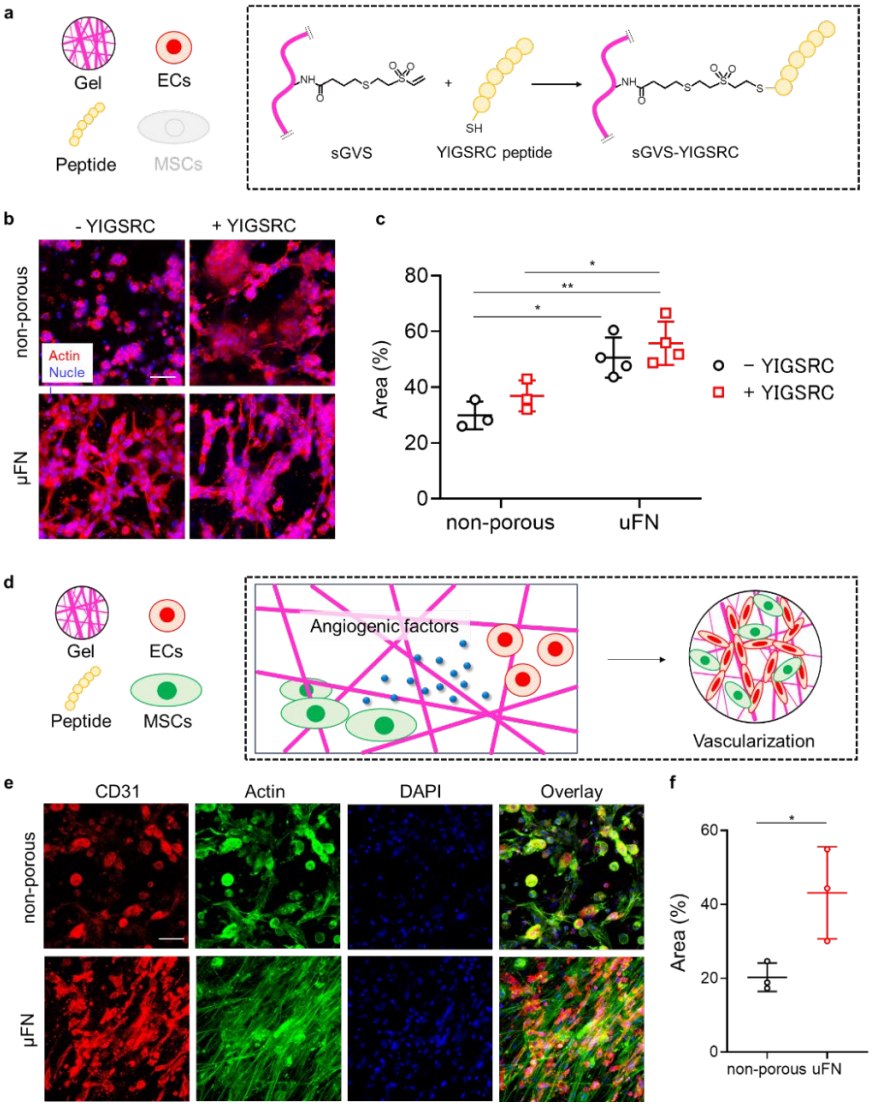

Figure 5. (a) Modification of μFN hydrogels with the laminin-mimetic YIGSRC peptide via thiol-ene reaction. (b) Effects of peptide modification and porous structures on the vascularization of ECs. ECs were encapsulated in hydrogels and cultured for 24 h. Actin and nuclei were stained with phalloidin (red) and DAPI (blue), respectively. (c) EC area was quantified using CLSM images (n=3). (d) Co-culture of ECs with mesenchymal stem cells (MSCs) in hydrogels for vascularization. (e) CLSM images of the co-culture of ECs with MSCs in non-porous and μFN hydrogels. CD31, actin, and nuclei were stained with the anti-CD31 antibody (red), phalloidin (green), and DAPI (blue), respectively. Phalloidin stained actin in both MSCs and ECs. (f) EC area was quantified using CLSM images (n=3). Data are represented as the mean ± SD from a representative experiment (biologically independent samples). *$P < 0.05$ and **$P < 0.01$ analyzed via one-way ANOVA with Tukey's multiple-comparison *post-hoc* test (c) and two-tailed Student's *t*-test (f). Scale bars represent 50 μm.

Conclusions

In this study, we developed microfibrous and microporous cell-encapsulating hydrogels for in vitro vascularization. FN hydrogels were prepared based on LLPS between tGUPy and HA and sequential gelation via thiol-ene chemical crosslinking. This bio-inspired supramolecular chemistry-based approach facilitated the control of matrix microstructures in hydrogels. Specifically, μFN hydrogels with tunable matrix microstructures enhanced tube formation by ECs via microporous structures. These hydrogels were further modified with laminin peptide and co-cultured with MSCs to enhance in vitro vascularization. In conclusion, our approach is useful to form new hydrogels with improved in vitro vascularization that can serve as hydrogel culture platforms for regenerative medicine and disease modeling applications.

AUTHOR INFORMATION

***Corresponding Author**

Akihiro Nishiguchi

E-mail: NISHIGUCHI.Akihiro@nims.go.jp

Author Contributions

A.N. designed and conducted the study. A.N. and E.A. performed the in vitro cell culture and microscopy. A.N., S.I., and D.P. conducted the animal experiments. A.N. wrote the manuscript. A. N. and T. T. edited the manuscript. All authors have reviewed the manuscript.

Notes/Conflict of Interest Disclosure

The authors declare no competing financial interest.

Data Availability Statement

All data generated/analyzed in this study are available upon request from the corresponding author.

ACKNOWLEDGEMENTS

This work received financial support from the Japan Society for the Promotion of Science (JSPS) KAKENHI (grant nos. 22H03962 and 23H01718), Uehara Memorial Foundation, and Inamori Foundation (Inamori Research Grants).

REFERENCES

1 O'Connor, C., Brady, E., Zheng, Y., Moore, E. & Stevens, K. R. Engineering the multiscale complexity of vascular networks. *Nat Rev Mater* **7**, 702-716 (2022).
2 Folkman, J. & Hochberg, M. Self-regulation of growth in three dimensions. *J Exp Med* **138**, 745-753 (1973).
3 Thomas, D., O'Brien, T. & Pandit, A. Toward customized extracellular niche engineering: Progress in cell-entrapment technologies. *Adv Mater* **30**, 1703948 (2018).
4 Song, W. *et al.* Engineering transferrable microvascular meshes for subcutaneous islet transplantation. *Nat Commun* **10**, 4602 (2019).
5 Brissova, M. & Powers, A. C. Revascularization of transplanted islets: can it be improved? *Diabetes* **57**, 2269-2271 (2008).
6 Emamaullee, J. A. & Shapiro, A. M. J. Factors Influencing the Loss of β-Cell Mass in Islet Transplantation. *Cell Transplant* **16**, 1-8 (2007).
7 Wang, X. *et al.* Composite Hydrogel Modified by IGF-1C Domain Improves Stem Cell Therapy for Limb Ischemia. *ACS Appl Mater Interfaces* **10**, 4481-4493 (2018).
8 Sekine, H. *et al.* In vitro fabrication of functional three-dimensional tissues with perfusable blood vessels. *Nat Commun* **4**, 1399 (2013).

9 Gaharwar, A. K., Singh, I. & Khademhosseini, A. Engineered biomaterials for in situ tissue regeneration. *Nature Reviews Materials* **5**, 686-705 (2020).
10 Nguyen, E. H. *et al.* Versatile synthetic alternatives to Matrigel for vascular toxicity screening and stem cell expansion. *Nat Biomed Eng* **1** (2017).
11 Wimmer, R. A. *et al.* Human blood vessel organoids as a model of diabetic vasculopathy. *Nature* **565**, 505-510 (2019).
12 Takebe, T. *et al.* Vascularized and functional human liver from an iPSC-derived organ bud transplant. *Nature* **499**, 481-484 (2013).
13 Baranski, J. D. *et al.* Geometric control of vascular networks to enhance engineered tissue integration and function. *Proc. Natl. Acad. Sci. U. S. A.* **110**, 7586-7591 (2013).
14 Bagrat Grigoryan *et al.* Multivascular networks and functional intravascular topologies within biocompatible hydrogels. *Science* **364**, 458–464 (2019).
15 Kim, S., Lee, H., Chung, M. & Jeon, N. L. Engineering of functional, perfusable 3D microvascular networks on a chip. *Lab Chip* **13**, 1489-1500 (2013).
16 Wang, Y., Kankala, R. K., Ou, C., Chen, A. & Yang, Z. Advances in hydrogel-based vascularized tissues for tissue repair and drug screening. *Bioact Mater* **9**, 198-220 (2022).
17 Kleinman, H. K. *et al.* Basement membrane complexes with biological activity. *Biochemistry* **25**, 312-318 (1986).
18 Aisenbrey, E. A. & Murphy, W. L. Synthetic alternatives to Matrigel. *Nat Rev Mater* **5**, 539-551 (2020).
19 Chan, V., Zorlutuna, P., Jeong, J. H., Kong, H. & Bashir, R. Three-dimensional photopatterning of hydrogels using stereolithography for long-term cell encapsulation. *Lab Chip* **10**, 2062-2070 (2010).
20 Han, L. H. *et al.* Microribbon-based hydrogels accelerate stem cell-based bone regeneration in a mouse critical-size cranial defect model. *J Biomed Mater Res A* **104**, 1321-1331 (2016).
21 Huebsch, N. *et al.* Matrix elasticity of void-forming hydrogels controls transplanted-stem-cell-mediated bone formation. *Nat Mater* **14**, 1269-1277 (2015).
22 Koh, J. *et al.* Enhanced In Vivo Delivery of Stem Cells using Microporous Annealed Particle Scaffolds. *Small* **15**, e1903147 (2019).
23 Moore, A. N. *et al.* Nanofibrous peptide hydrogel elicits angiogenesis and neurogenesis without drugs, proteins, or cells. *Biomaterials* **161**, 154-163 (2018).
24 Nishiguchi, A. *et al.* Injectable microcapillary network hydrogels engineered by liquid-liquid phase separation for stem cell transplantation. *Biomaterials* **305**, 122451 (2024).
25 Brigitte J. B. Folmer, Rint P. Sijbesma, Ron M. Versteegen, Joost A. J. van der Rijt & Meijer, E. W. Supramolecular polymer materials: Chain extension of telechelic polymers using a reactive hydrogen-bonding synthon. *Adv. Mater.* **12**, 874-878 (2000).
26 Nishiguchi, A., Ichimaru, H., Ito, S., Nagasaka, K. & Taguchi, T. Hotmelt tissue adhesive with supramolecularly-controlled sol-gel transition for preventing postoperative abdominal adhesion. *Acta Biomater.* **146**, 80-93 (2022).
27 Zhao, H. & Heindel, N. D. Determination of degree of substitution of formyl groups in polyaldehyde dextran by the hydroxylamine hydrochloride method. *Pharm. Res.* **8**, 400-402 (1991).
28 Dankers, P. Y., Harmsen, M. C., Brouwer, L. A., van Luyn, M. J. & Meijer, E. W. A modular and supramolecular approach to bioactive scaffolds for tissue engineering. *Nat. Mater.* **4**, 568-574 (2005).

29 Wolf, K. J. & Kumar, S. Hyaluronic Acid: Incorporating the Bio into the Material. *ACS Biomater. Sci. Eng.* **5**, 3753-3765 (2019).
30 Abbas, M., Lipinski, W. P., Wang, J. & Spruijt, E. Peptide-based coacervates as biomimetic protocells. *Chem. Soc. Rev.* **50**, 3690-3705 (2021).
31 Jun, H. W. & West, J. Development of a YIGSR-peptide-modified polyurethaneurea to enhance endothelialization. *J Biomater Sci Polym Ed* **15**, 73-94 (2004).
32 Han, Y. *et al.* Mesenchymal Stem Cells for Regenerative Medicine. *Cells* **8** (2019).

Table of Contents (TOC)/Abstract Graphic